Since January 2020 Elsevier has created a COVID-19 resource centre with free information in English and Mandarin on the novel coronavirus COVID-19. The COVID-19 resource centre is hosted on Elsevier Connect, the company's public news and information website.

Virus Research 283 (2020) 197974

Contents lists available at ScienceDirect

Virus Research

journal homepage: www.elsevier.com/locate/virusres

Involvement of VCP/UFD1/Nucleolin in the viral entry of *Enterovirus A* species

Jingjing Yan[a,1], Meng Wang[a,1], Min Wang[a], Ying Dun[a], Liuyao Zhu[a], Zhigang Yi[b,*], Shuye Zhang[a,*]

[a] Shanghai Public Health Clinical Center and Institutes of Biomedical Sciences, Fudan University, Shanghai, China
[b] Department of Pathogen Diagnosis and Biosafety, Shanghai Public Health Clinical Center, Fudan University, Shanghai, China

ARTICLE INFO

Keywords:
Enterovirus A71
VCP
UFD1
Plus-stranded RNA virus
Virus entry

ABSTRACT

Valosin-containing protein (VCP) plays roles in various cellular activities. Recently, Enterovirus A71 (EVA71) infection was found to hijack the VCP protein. However, the mechanism by which VCP participates in the EVA71 life cycle remains unclear. Using chemical inhibitor, RNA interference and dominant negative mutant, we confirmed that the VCP and its ATPase activity were critical for EVA71 infection. To identify the factors downstream of VCP in enterovirus infection, 31 known VCP-cofactors were screened in the siRNA knockdown experiments. The results showed that UFD1 (ubiquitin recognition factor in ER associated degradation 1), but not NPL4 (NPL4 homolog, ubiquitin recognition factor), played critical roles in infections by EVA71. UFD1 knockdown suppressed the activity of EVA71 pseudovirus (causing single round infection) while it did not affect the viral replication in replicon RNA transfection assays. In addition, knockdown of VCP and UFD1 reduced viral infections by multiple human *Enterovirus A* serotypes. Mechanistically, we found that knockdown of UFD1 significantly decreased the binding and the subsequent entry of EVA71 to host cells through modulating the levels of nucleolin protein, a coreceptor of EVA71. Together, these data reveal novel roles of VCP and its cofactor UFD1 in the virus entry by EVA71.

1. Introduction

Enterovirus, single-stranded positive-sense RNA virus, belongs to the *Picornaviridae* family *Enterovirus* genus. The *Enterovirus* genus consists of 12 species, including *Enterovirus A* (Enterovirus A71, Coxsackievirus A6, A10, A16 *etc.*), *B* (Coxsackievirus B3, CVB3 *etc.*), *C* (Poliovirus, *etc.*), *D* (Enterovirus D68 *etc.*) species and *Rhinovirus A, B, C etc.* (Walker et al., 2019). Enterovirus A71 (EVA71) and Coxsackievirus A16 (CVA16) are the major causative pathogen of hand, food and mouth disease (HFMD). Recently, HFMD associated with Coxsackievirus A6 and A10 (CVA6 and CVA10) also emerged (Aswathyraj et al., 2016). In China, EVA71 caused a severe HFMD outbreak in 2008, and HFMD has since become epidemic (Zhang et al., 2010). No effective therapy is currently available for HFMD and more studies are needed to elucidate the mechanisms of enterovirus infection and HFMD pathogenesis.

EVA71 is a non-enveloped virus and has an icosahedral shell with a canyon around the five-fold axes as the binding site for virus receptor (Plevka et al., 2012; Wang et al., 2012). The human scavenger receptor class B, member 2 (SCARB2) was found to be the exclusive receptor to induce uncoating of EVA71 *in vitro* (Yamayoshi et al., 2009). SCARB2 binds EVA71 on the southern rim of the canyon (Zhou et al., 2019) and expelles the pocket factor from the EVA71 virion, hence destabilizing the capsid and triggering the uncoating process (Dang et al., 2014). In addition, other host factors on the cell surface are reported to facilitate EVA71 entry, such as Annexin A2, fibronectin, vimentin and nucleolin (Du et al., 2014; He et al., 2018; Su et al., 2015; Yang et al., 2011). These receptors were identified as binding receptors to capture EVA71 on the cell surface.

The genome of EVA71 encodes eleven proteins, including four viral capsid proteins (VP1-VP4) and seven non-structure proteins (2A-2C, 3A-3D) (Huang et al., 2012). The viral RNA-dependent RNA polymerase

Abbreviations: EVA71, Enterovirus A71; CVA6, Coxsackievirus A6; CVB3, Coxsackievirus B3; PV, Poliovirus; VCP, Valosin-containing protein; UFD1, ubiquitin recognition factor in ER associated degradation 1; NPL4, NPL4 homolog, ubiquitin recognition factor; SRIPs, single round infectious particles; GuHCl, Guanidine Hydrochloride; ERAD, endoplasmic reticulum associated degradation; siRNA, small interfering RNA

* Corresponding authors.
E-mail addresses: zgyi@fudan.edu.cn (Z. Yi), zhangshuye@shphc.org.cn (S. Zhang).
[1] Co-first author.

https://doi.org/10.1016/j.virusres.2020.197974
Received 9 February 2020; Received in revised form 8 April 2020; Accepted 8 April 2020
Available online 11 April 2020

$3D^{pol}$ and 3AB, 2C assemble into the viral replication organelles (ROs) (Baggen et al., 2018). Various host RNA-binding proteins are also involved in viral genome replication, including poly(rC)-binding protein 2 (PCBP2), polyadenylate-binding protein 1 (PABP1) and heterogeneous nuclear ribonucleoprotein C (HNRNPC) (Baggen et al., 2018; Owino and Chu, 2019). Replication occurs on virus-induced, tubulovesicular ROs, which are derived from endoplasmic reticulum (ER) and/or Golgi apparatus membranes (Baggen et al., 2018; Owino and Chu, 2019). Valosin-containing protein (VCP), a hexameric type II AAA ATPase, participates in various cellular activities including protein homeostasis, DNA replication and repair and autophagy (Meyer and Weihl, 2014). VCP has been found to play roles in replication of poliovirus and Hepatitis C virus (Arita et al., 2012; Yi et al., 2016), and originally identified as host factor of Drosophila C virus(Cherry et al., 2006). Recently, VCP was identified to be required in EVA71 replication (Wu et al., 2016) and VCP co-exists with the viral protein and other known replication-related molecules in EVA71-induced ROs (Wang et al., 2017). However, the precise mechanism of VCP involved in EVA71 life cycle remains elusive.

VCP encompasses a N-terminal domain, two highly conserved ATPase domains and an unstructured C-terminal tail. This enzyme hydrolyzes ATP and utilizes the energy to extract protein subunit or disassemble protein complexes from protein assemblies, chromatin and membranes (DeLaBarre and Brunger, 2003). The activity of VCP is tightly controlled by various regulatory cofactors, which either associate with the N-terminal domain or interact with the C-terminus *via* distinct binding motifs and target VCP to specific cellular pathways (Hanzelmann and Schindelin, 2017). Based on their functions, cofactors are divided into three major classes: (i) Substrate-recruiting cofactors like UBA-UBX proteins and UFD1-NPL4 which bring substrates to VCP; (ii) Substrate processing cofactors like ubiquitin (E3) ligases, deubiquitinases (DUBs) and peptide N-glycanase (PNGase); (iii) Regulatory cofactors like UBX proteins UBXD4 and ASPL as well as SVIP (Hanzelmann and Schindelin, 2017). VCP cofactors interact with VCP *via* several conserved binding motifs (Buchberger et al., 2015). Majority of cofactors interact with the VCP N-terminal domain either *via* the ubiquitin regulatory X (UBX)/UBX-like (UBXL) domain or three linear binding motifs, called VCP-interacting motif (VIM), VBM (VCP-binding motif), and SHP (BS1, binding segment), whereas other cofactors bind to VCP *via* their PNGase/UBA or UBX containing proteins (PUB) or PLAP, Ufd3p, and Lub1p (PUL) domain to the C-terminal tail of VCP.

In this study, we found that VCP was involved in both pre-entry and post-entry stages of EVA71 life cycle. In contrast, UFD1, a cofactor of VCP, facilitated viral entry. Knockdown of UFD1 significantly reduced the binding of EVA71 to host cells, but had no effect on viral RNA replication. Moreover, UFD1 regulates the viral co-receptor nucleolin expression since knockdown of UFD1 significantly reduces the expression of nucleolin, leading to decreased binding of EVA71 to host cells. Thus, our study reveals novel mechanisms of VCP and its cofactors to facilitate enterovirus infection.

2. Materials and methods

2.1. Cells and viruses

Human rhabdomyosarcoma (RD) cells, human cervical epithelial Hela cells and human hepatoma epithelial cells Huh-7 were cultured in Dulbecco's modified Eagle's medium (DMEM) supplemented with 10 % fetal bovine serum (FBS, Gibco, Waltham, MA, USA), 100U/mL penicillin and 100 μg/mL streptomycin. All the cell lines were purchased from the Cell Bank of the Chinese Academy of Sciences (Shanghai, China). EVA71 strain (KU936132), Coxsackievirus A6 (KX064292) and Coxsackievirus A16 (MG957117) isolated in Shanghai were kindly provided by Dr. Yunwen Hu. The Coxsackievirus A10 prototype strain (AY421767) was rescued from an infectious clone constructed in our laboratory. Coxsackievirus B3 (Nancy strain) was from Dr. Chunsheng Dong (Wu et al., 2018). Poliovirus containing an in-frame fused GFP in the 2A protein was generated from an infectious clone described previously (Du et al., 2018). Viruses were propagated in RD cells. Viral titers were determined in RD cells by plaque assay.

2.2. Antibodies and reagents

Mouse monoclonal antibody against EVA71 capsid protein VP-1 was purchased from Abcam (Cambridge, UK). EVA71 2C and 3C were from GeneTex (Irvine, CA, USA), and used in Western-blot detection of the respective proteins. Rabbit anti-VCP antibody was from ABclonal (Wuhan, China). Rabbit polyclonal antibodies against human UFD1 and NPL4 were purchased from Proteintech (Chicago, IL, USA). Rabbit monoclonal antibodies against human Annexin A2, vimentin and nucleolin were from Cell Signaling Technologies (Danvers, MA, USA). Goat anti-SCARB2 antibody was from R&D systems (Minneapolis, MN, USA). The J2 anti-dsRNA IgG2a monoclonal antibody was obtained from SCICONS (Budapest, Hungary). The secondary antibody conjugated to Allophycocyanin (APC) was from BD Biosciences (Franklin Lakes, CA, USA). Horseradish peroxidase (HRP)-conjugated anti-goat IgG was from Qcbio S&T (Shanghai, China). AlexaFluor680-conjugated anti-rabbit IgG was from Jackson ImmunoResearch (West Grove, PA, USA) and AlexaFluor790-conjugated anti-mouse IgG was from Jackson ImmunoResearch. AlexaFluor594-Conjugated AffiniPure Goat Anti-Mouse IgG (H + L) was from ZSGB-BIO (Beijing, China). Fluoroshield Mounting Medium with DAPI was from Abcam. NMS-873 was purchased from Selleck (Shanghai, China). Guanidine hydrochloride (GuHCl) was from MedChem Express (Monmouth Junction, NJ, USA). All drugs were prepared according to the manufacturer's instructions under sterile conditions. Luciferase assay system was from Promega (Madison, WI, USA). Wheat germ agglutinin (WGA)-conjugated with AlexFluor488 was from ThermoFisher Scientific (MA, USA).

2.3. Plasmid

The pLKO.1 based short hairpin RNA (shRNA) plasmids and pTRIP-BSD-VCP-es and the dominant negative mutant contrast pTRIP-BSD-VCP-es-DN (E305Q/E578Q) plasmids were previously described (16). The DNA fragments encoding the ASPL-C (residues 313-553) and ASPL-C PP 437-438 AA were synthesized (GENEWIZ, Suzhou, China) and cloned into pcDNA6.0-EGFP backbone by seamless cloning (Qcbio S&T, Shanghai, China). The pcDNA6.0-EGFP plasmid was used as a control.

2.4. Cell viability assay

Cell viability upon inhibitors treatment was assessed by employing the cell counting kit-8 (CCK-8, Dojindo Laboratories, Kumamoto, Japan). Briefly, cells were seeded in 96-well cell culture plates and subsequently treated with chemical inhibitors for 6 h before incubation with 10 μL CCK-8 for 20 min at 37 °C. The absorbance at a wavelength of 450 nm was determined and plotted.

2.5. Small RNA interference

The siRNAs for 31 VCP cofactors (3 siRNAs per gene) and scrambled siRNA were purchased from Gene Pharma (Shanghai, China). The sequences of siRNA were available upon request. All transfections were performed in a 12-well plate format. The procedure was performed as previously described (Yuan et al., 2018). The gene knockdown efficiency was determined by real-time qRT-PCR at 48 h and by Western blotting at 72 h. The experiments of EVA71 infection were conducted at day 3 post siRNA transfection.

2.6. Monitoring viral infectivity by Flow cytometry

EVA71 infected cells were trypsinized with 0.25 % trypsin-EDTA

and then collected for intracellular staining. Harvested cells were washed with PBS containing 1% FBS, and then permeabilized with Fixation/Permeabilization solution (BD Biosciences) for 20 min. After washing with 1 × BD Perm/Wash buffer, cells were incubated with the mouse anti-EVA71 VP-1 antibody (diluted by 1:1000) at room temperature for 40 min. Then cells were stained with APC-conjugated rat anti-mouse IgG1 for 30 min. Finally, cells were resuspended in Perm/Wash buffer and analyzed by BD Accuri C6 (BD Biosciences).

2.7. Plaque assay

RD cells were seeded in 6-well or 12-well plate and incubated overnight. The virus stocks were serially diluted 10-fold (10^{-3}-10^{-7}) with 2%FBS/DMEM and allowed to absorb onto confluent cells for 1 h at 37 °C. The inoculum was then removed, and cells were washed three times with PBS and then covered with 1% agar medium. After 4 days of incubation, the cells were fixed and stained with 1% crystal violet and plaques were counted. The virus titers were calculated as PFU/mL.

2.8. EVA71 single round infection system

The plasmids of EVA71 subgenomic replicon and EVA71 capsid were kindly provided by Prof. Wenhui Li from National Institute of Biological Sciences, Beijing (Chen et al., 2012). EVA71 replicon construct contains all the gene segments of EVA71 except the capsid portion which is replaced by the firefly luciferase or EGFP (referred as EVA71-Luc or EVA71-EGFP). The replicon RNAs of EVA71-Luc or EVA71-EGFP were obtained from the linearized plasmid by *in vitro* transcription. The pseudotyped viruses were produced by sequential transfection of capsid plasmid and replicon RNA into HEK293 T cells as described previously (Yuan et al., 2018). RD cells transfected with siRNA against VCP, UFD1 and NPL4, were seeded in 24-well plates. The next day, cells were pretreated with DMSO or GuHCl (2μM) for 30 min and then infected with pseudovirus or transfected with replicon RNA of EVA71-Luc. Luciferase activity was measured at indicated time points. In the EVA71-EGFP replicon experiment, the siRNA transfected RD cells were infected with pseudovirus or transfected with EVA71-EGFP replicon RNA. The expression of EGFP was detected by fluorescence microscopy and flow cytometry at 12 h post infection or transfection.

2.9. EVA71-AlexaFluor594 labeling

EVA71 was concentrated by ultracentrifugation at 120,000 *g* for 4 h at 4 °C (SW32Ti rotor, Beckman Coulter Optima L-100XP). The viral titer of the concentrated EVA71 was measured by plaque assay. Then 3×10^8 PFU of EVA71 was labeled with Alexa Fluor™ 594 NHS Ester (A37572, ThermoFisher) following the instruction of the manuscript. The labeled EVA71 was aliquoted and stored at −80 °C, and the titer was measured by plaque assay.

2.10. Virus binding and entry assay by qPCR

Following transfection with NC, VCP, UFD1 or NPL4 siRNA for 2 days, RD cells were seeded to 24-well plates (2×10^5 cells/well) and incubated for 24 h. The cells were treated with binding buffer (HBSS supplied with 1% BSA) for 10 min and then incubated with EVA71 at an MOI of 10 for 2 h at 4 °C (binding) or 37 °C (entry). Then cells were washed with cold PBS three times to remove unbound viruses. Total RNA was then extracted using the RNA purification kit (TIANGEN, Beijing, China). Reverse transcriptions were then carried out using the HiScript II first strand cDNA synthesis kit (Vazyme, Nanjing, China). SYRB Green-based qPCR was performed on the LineGene 9600 Plus (Hangzhou Bioer, China) using SYRB Green qPCR Master Mix (Hangzhou Bioer, China). The primers for EVA71 and h18 s quantification were as follows: EVA71-F: 5′- GCAGCCCAAAACAACTTCAC-3′, EVA71-R: 5′- AAT TTCAGCAGCTTGGAGTGC-3′; h18s-F: 5′- GTAACCC GTTGAACCCCATT-3′, h18s-R: 5′-CCATCCAATCGGTAGTAGCG-3′.

2.11. Viral binding and entry assay by immunofluorescence

Following transfection with NC, VCP, UFD1 or NPL4 siRNA for 2 days, RD cells were seeded to 12-well plates (3×10^5 cells/well) with coverslips. The next day, RD cells were treated with binding buffer (HBSS supplied with 1% BSA) for 10 min and then incubated with EVA71 labeled with AlexaFluor594 at an MOI of 10 at 4 °C (binding) or 37 °C (entry) for 2 h. After extensive wash, cells were stained with Wheat germ agglutinin (WGA) conjugated to AlexaFluor488 to label cell membrane. After three times washes with HBSS, coverslips were applied to mounting medium with DAPI. Digital confocal images were collected with TCS SP5 II Confocal Microscope (Leica, Buffalo Grove, IL, USA).

2.12. Western blotting

Cells were first harvested and then lysed in Radioimmunoprecipitation assay buffer (RIPA buffer, 50 mM Tris, 150 mM NaCl, 1% Trition X-100, 1% sodium deoxycholate, 0.1 % SDS and 2.5 mM EDTA) with a mixture of protease inhibitors (ThermoFisher). The concentration of proteins was quantified by bicinchoninic acid (BCA) protein assay. Equal amounts of proteins were loaded and separated by SDS-PAGE, and then transferred to a nitrocellulose membrane. The membrane was blocked with 0.1 % Tween-20 in PBS containing 5% BSA and then incubated overnight with primary antibodies at 4 °C. After three times washes with 0.1 % Tween-20/PBS, the membrane was incubated with HRP or fluorophore conjugated secondary antibodies for 1 h at room temperature. The immunoblots were visualized using an Odyssey Fc Imager (Lincoln, NE, USA).

2.13. Statistical analysis

Significance of differences was evaluated using paired Student's *t* test. Statistical analysis was performed with GraphPad Prism version 7.0 (La Jolla, CA, USA).

3. Results

3.1. VCP is critical for EVA71 infection

To explore the role of VCP in EVA71 replication cycle, we first used NMS-873, a pharmacological inhibitor of VCP (Magnaghi et al., 2013) to assess its effect on viral replication. We treated RD cells with various concentration of NMS-873 and assessed the viral replication by monitoring the intracellular level of viral capsid protein VP-1. NMS-873 treatment reduced viral replication in a dose-dependent manner, evidenced by decreased levels of viral capsid protein VP-1 (Fig. 1a and b) with only marginal loss (< 20 %) of cell viability at the highest dosage (Fig. 1b). The inhibitory effects of NMS-873 were also verified by plaque assay to monitor the virion production and by western blotting to monitor the expression level of viral proteins. (Fig. 1c and d)

To further confirm the requirement of VCP in EVA71 infection, we performed shRNA-medicated knockdown of VCP. There were reduced viral replication, evidenced by reduction of the intracellular VP-1 protein (Fig. 1e) and viral production (Fig. 1f) in the VCP-knockdown cells. Western blot showed that transfection of shVCP decreased the expression of VCP, compared with shNC. Moreover, knockdown of VCP dramatically reduced EVA71 infection, as assessed by flow cytometry and plaque assay (Fig. 1e and f). These data indicate a critical role of VCP in EVA71 infection.

3.2. The ATPase activity of VCP is required in EVA71 infection

VCP contains two ATP-binding (AAA) domains. Double mutation

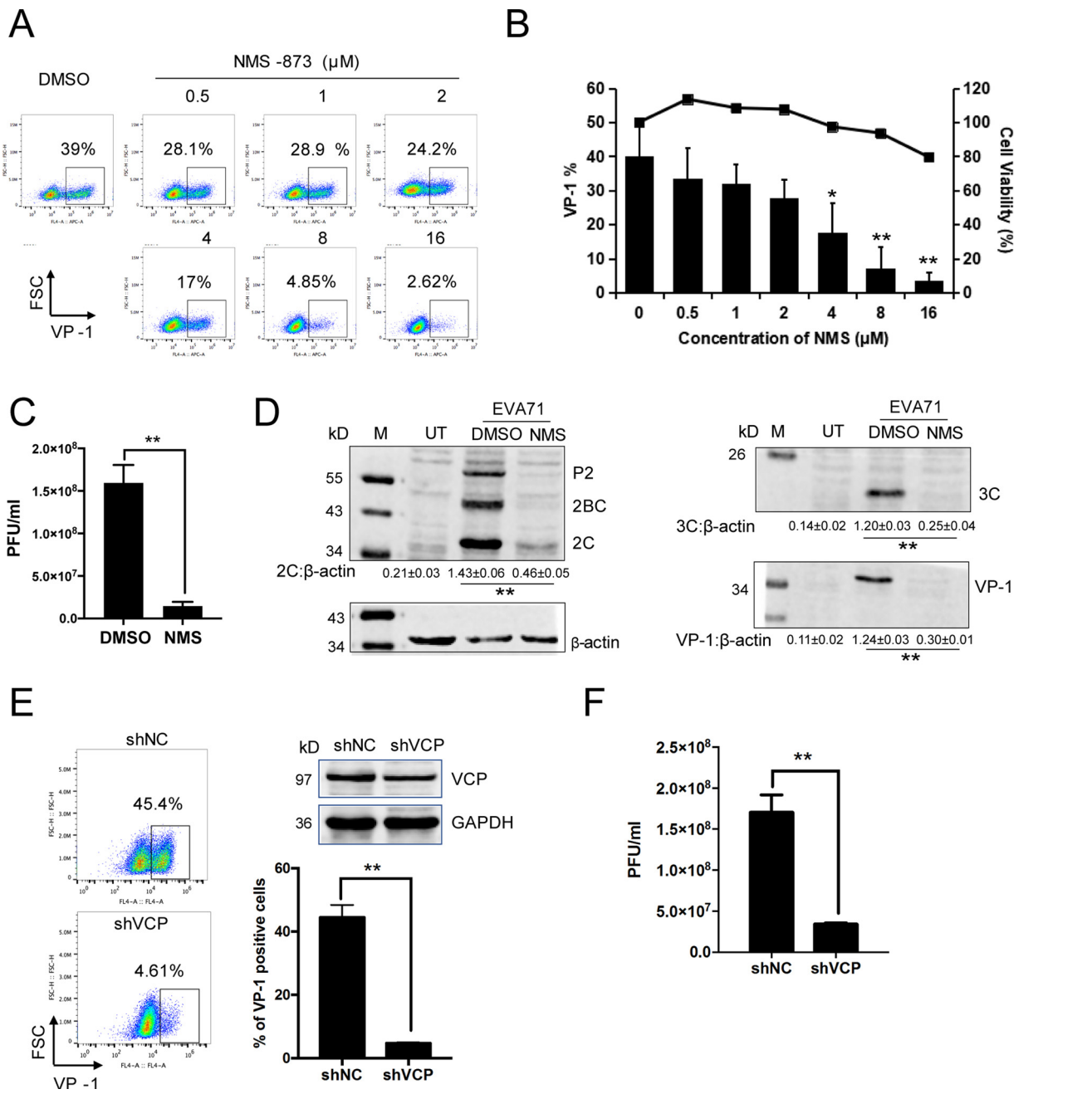

Fig. 1. VCP plays an important role in EVA71 infection.

A. RD cells were pretreated with increasing concentrations of VCP inhibitor – NMS 873 for 1 h. Then EVA71 was added at an MOI of 1 for 6 h. The infected cells were processed for flow cytometry. The typical VP-1 expression data was shown. B. The bar charts represented the EVA71 infectivity determined by the percentage of VP-1 positive cells and were shown (means ± SD, n = 3). Cell viability upon NMS-873 treatments was shown by the curve above the chart. C–D. RD cells were pretreated with DMSO or NMS-873 (8 μM) for 1 h and then EVA71 (MOI = 1) was added. After internalization within 1 h, EVA71 was removed and cells were washed with PBS for three times. 12 h later, the supernatants were collected for plaque assay (means ± SD, n = 3) (C) and the cells were lysed for Western blot (D). E–F. RD cells were transfected with shNC or shVCP vectors. The levels of VCP expression were measured by WB (E). After 48 h, cells were infected with EVA71 at an MOI of 1 for 6 h. The infectivity was determined by flow cytometry (E). The bar chart showed the summary of three independent experiments (means ± SD) (E). The plaque assay was used to measure viral titers (means ± SD, n = 3) (F). UT, untreated cells; PFU, plaque forming unit. Statistical significance was determined by Student's *t* test Student's *t* test. *, $p < 0.05$; **, $p < 0.01$.

(E305Q/E578Q) of these two domains completely abolishes ATPase activity, as a dominant negative mutant (Yi et al., 2016). To determine whether the ATPase activity of VCP is required for EVA71 replication, we performed a rescue experiment by co-transfection of shRNA against VCP and overexpression of shRNA-resistant VCP (VCP-es) or dominant negative mutant VCP (VCP-es-DN). As shown in Fig. 2a and b, VCP-es could restore EVA71 infection, and VCP-es-DN synergistically reduced EVA71 infection, demonstrating that ATPase activity of VCP is critical for the infection.

Alveolar soft part sarcoma locus (ASPL), a cofactor of VCP with high-affinity, is reported to promote VCP hexamer disassembly and disrupt the D2 ATPase activity of VCP (Arumughan et al., 2016). Its extended UBX domain-containing fragment (residues 313-553, termed ASPL-C), is critical for the interaction with VCP, while its mutant (two Proline amino acids of residues 437-438 were replaced by two Alanine amino acids, termed ASPL-C PP 437-438 AA) loses the binding for VCP

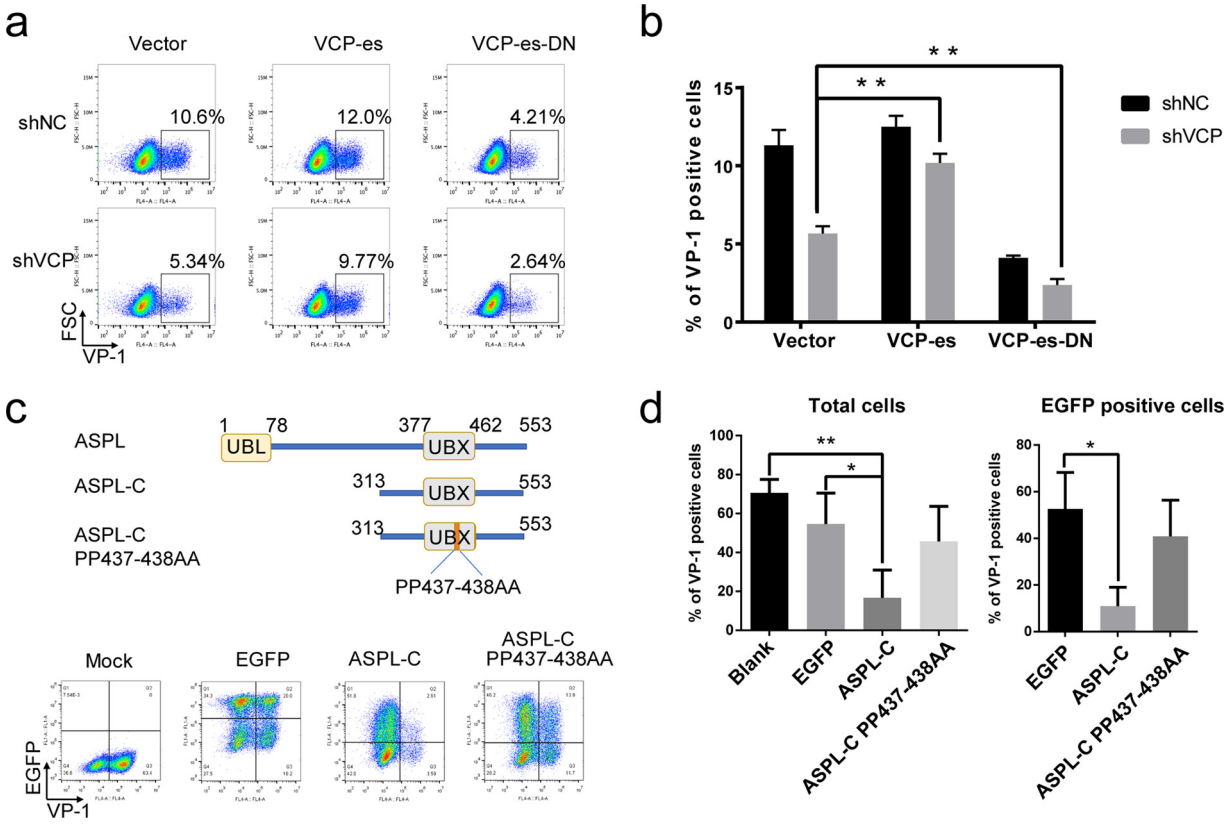

Fig. 2. The ATPase activity of VCP is required in EVA71 infection.
A–B, RD cells were co-transfected with shNC or shVCP and vector, VCP-es (shRNA escape), VCP-es-DN. After 48 h transfection, cells were infected with EVA71 at an MOI of 1 for 6 h. The representative figure of flow cytometry was shown (A). The three independent experiments were summarized in the right panel (means ± SD) (B). C–D. Schematic representation of fragments and full length ASPL. Conserved protein domains are depicted: ubiquitin-like domain (UBL); ubiquitin regulatory-X domain (UBX). RD cells were transfected with EGFP, ASPL-C, ASPL-C PP 437-438 AA. After 48 h, cells were infected with EVA71 at an MOI of 1 for 6 h. The representative figure of flow cytometry was shown (C). The three independent experiments were summarized in the right panel (means ± SD) (D). Statistical significance was determined by Student's *t* test Student's *t* test. *, $p < 0.05$; **, $p < 0.01$.

(Arumughan et al., 2016). Therefore, we constructed the ASPL-C and ASPL-C PP 437-438 AA to further assess the necessity of VCP's enzymatic activity. Our results showed that the overexpression of ASPL-C, which disrupts VCP activity, could dramatically reduce EVA71 infection; while the overexpression of mutant PP 437-438 AA, which did not bind VCP, had little effect on the EVA71 infection (Fig. 2c and d).

3.3. The cofactor UFD1 but not NPL4 of VCP is critically involved in EVA71 infection

VCP itself barely exhibits substrate specificity. It engages a large number of cofactors for its diverse functions (Buchberger et al., 2015). To identify which cofactors of VCP are involved in EVA71 infection, we screened with siRNAs targeting 31 reported VCP-interacting proteins. Knockdown of majority of these cofactors had marginal effect on EVA71 infection, despite of effective knockdown of the targeted genes (Fig. 3a). However, the siRNAs against UBXN6, UFD1 and SPRTN significantly reduced the viral infectivity (Fig. 3b). Since UFD1 interference showed the most consistent and the largest suppressing effect, we subsequently focused on the role of UFD1 in virus infection. To exclude the off-target effects of siRNA against UFD1, we examined three siRNA oligosaccharides and two previously reported oligosaccharides showing strong suppressing effects individually. The data showed that the EVA71 infectivity negatively correlated with the remaining UFD1 levels in infected RD cells, confirming a requirement of UFD1 for efficient viral infection (Fig. 3c and d). UFD1 is known to be a partner of NPL4 in the VCP machinery to function in various protein quality control processes, for example, facilitating the translocation of misfolded protein from ER to the cytosol during the ER associated degradation (Ye et al., 2003). However, knockdown of NPL4 did not affect EVA71 infection in our screening and the subsequent confirmatory experiments (Fig. 3e). In conclusion, we found that knockdown of VCP and UFD1 but not NPL4 could significantly reduce EVA71 infection, indicating a likely novel working mechanism of VCP-UFD1 in facilitating EVA71 infection without NPL4.

3.4. UFD1 facilitates the infection of Enterovirus A species

To investigate whether the observed effect of UFD1 in EVA71 infection is exclusive in RD cells, we assayed the viral infections in Hela and Huh7 cells. UFD1 knockdown significantly suppressed EVA71 infection compared with the siRNA control. In contrast, NPL4 siRNA had little effects on virus infection in both Hela and Huh7 cells (Fig. 4a and b). Next, we examined the infection by other viral serotypes of *Enterovirus A* species, including CVA16, CVA6 and CVA10. Interestingly, the infection of all three viral types was inhibited after knockdown of VCP and UFD1, shown as the significantly diminished viral dsRNA staining (Fig. 4c and d). In addition, we performed plaque assay to monitor the effects of knocking down VCP and UFD1. The data confirmed that siRNA of VCP significantly reduced the infection by EVA71, CVA16, CVA6 and CVA10, while siRNA of UFD1 reduced virus titers of EVA71 and CVA16, although the inhibitory effects on CVA6 and CVA10 did not reach statistical significance in current experimental settings (Fig. 4e).

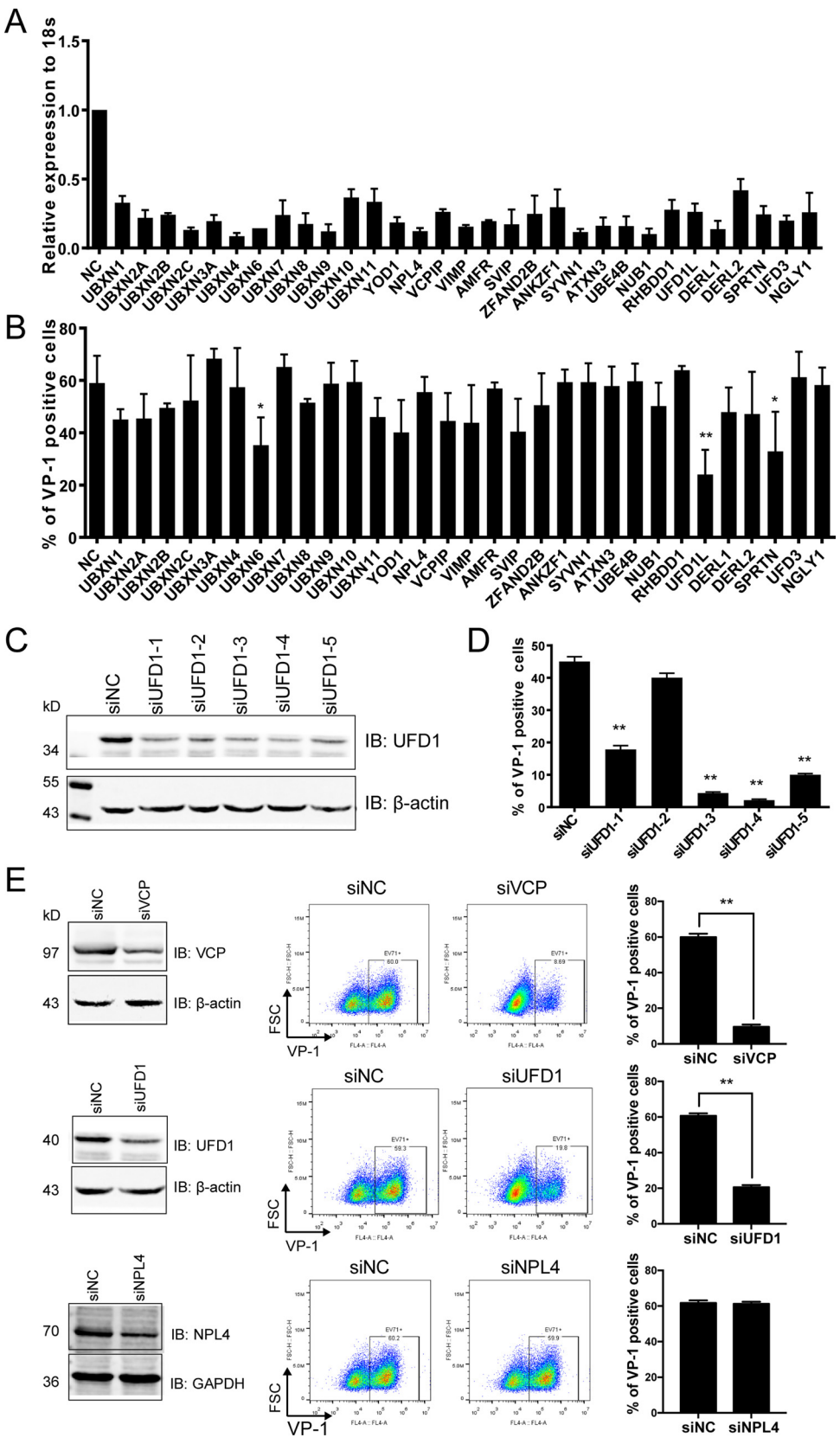

Fig. 3. The cofactor UFD1 but not NPL4 of VCP is critically involved in EVA71 infection.
A–B. RD cells were transfected by siRNA pools of the 31 VCP cofactors (3 siRNAs per gene), respectively. At day 3, cells were infected with EVA71 at an MOI of 1 for 6 h. The RNA levels of these 31 genes were measured by qPCR after 72 h transfection (A). The percentage of VP-1 positive cells were detected by flow cytometry (B). Three independent experiments with means ± SD were shown. C–D. RD cells were transfected with each UFD1 siRNA of the pool (UFD1-1, 2, 3) and another two reported siRNAs (UFD1-4, 5). 3 days later, cells were lysed and probed by anti-UFD1 antibody. β-actin was used as an internal control (C). After EVA71 infection for 6 h, VP-1 was detected by flow cytometry (means ± SD, n = 3) (D). E. RD cells were transfected with siRNA against VCP, UFD1 and NPL4. After 3 days, the protein levels were determined by western blotting, and the infectivity was measured by flow cytometry. One representative result of three independent experiments was shown. The three independent experiments were summarized in the right panel (means ± SD). Statistical significance was determined by Student's *t* test Student's *t* test. *, $p < 0.05$; **, $p < 0.01$.

3.5. UFD1 targets viral entry step but not replication during viral life cycle

To further study how VCP and UFD1 interact with the enterovirus life cycle, we performed the time of addition assay testing the VCP inhibitor (NMS-873). We found that early inhibition of VCP led to more viral inhibition shown by less VP-1 levels, EVA71 RNA and viral yields, indicating the involvement of VCP in early steps of viral infection (Fig. 5a–c).

To explore the involvement of VCP and UFD1 in different stages during enterovirus life cycle, their roles in viral replications were

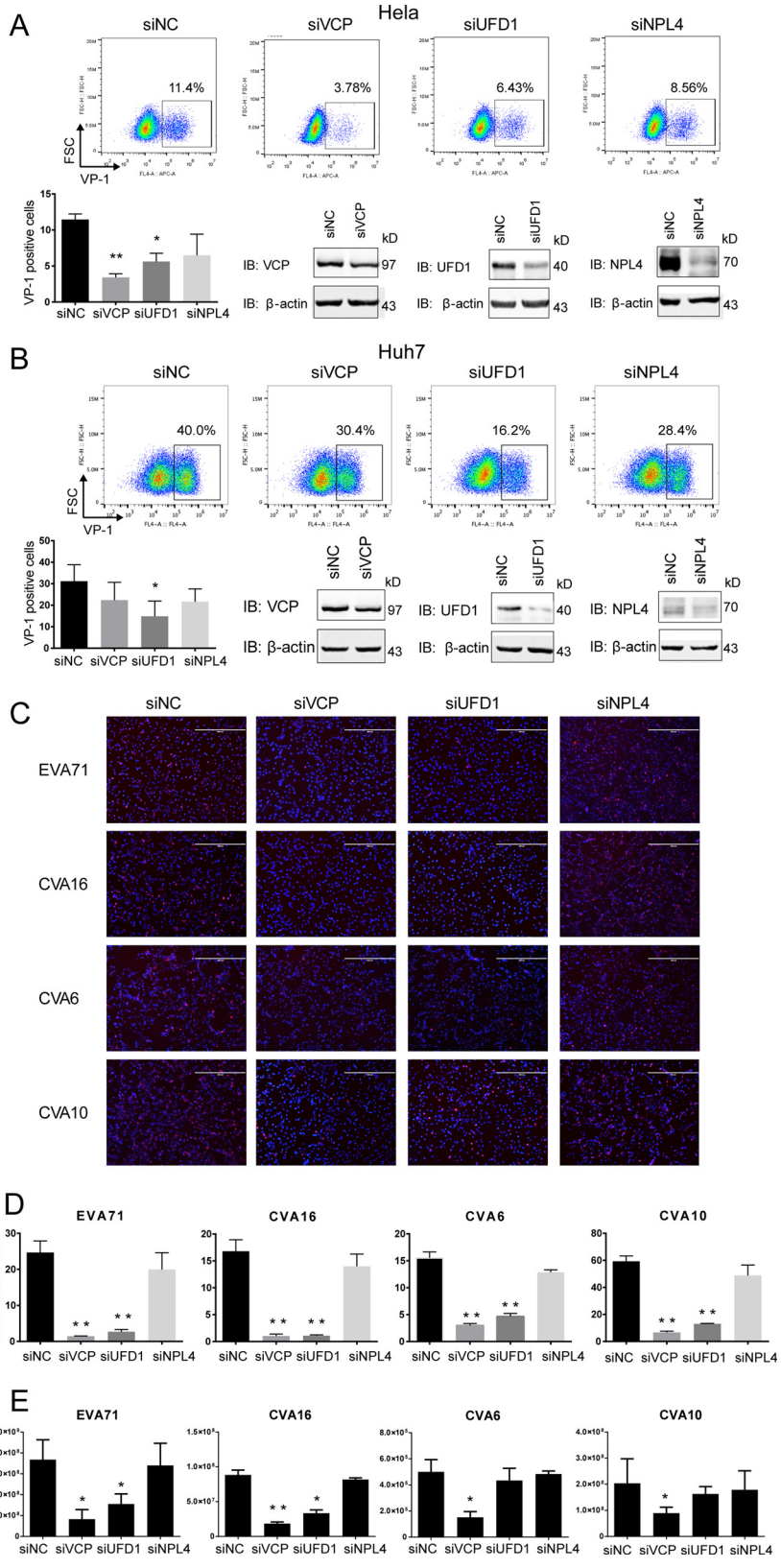

Fig. 4. UFD1 facilitates the infection of *Enterovirus A* species. A–B. Hela (A) and Huh7 (B) cells were transfected with siRNA against VCP, UFD1 and NPL4. siNC was used as negative control. After 3 days, the percentages of VP-1 positive cells were measured by flow cytometry and the protein levels were determined by western blotting. The bar chart showed the summary data (means ± SD, n = 3). C. RD cells were transfected with siRNA against VCP, UFD1 and NPL4. siNC was used as negative control. After 72 h, cells were infected with EVA71, CVA16, CVA6 and CVA10 at an MOI of 1 for 4 h. Cells were washed and then fixed and stained with anti-dsRNA (J2 antibody). Then anti-mouse IgG conjugated with Alex Fluor594 was incubated. DAPI was used to visualize the nuclei. (dsRNA, red; nuclei, blue). D. The percentage of infected cells was counted and summarized (means ± SD, 5 microscopic fields). E. After gene knockdown, cells were replated in 12 well plates. The next day, cells were incubated with serially diluted EVA71, CVA16, CVA6 and CVA10 for 1 h. Then plaque assay was performed (means ± SD, n = 3). Statistical significance was determined by Student's *t* test Student's *t* test. *, $p < 0.05$; **, $p < 0.01$.

examined in enterovirus replicon RNAs transfection assays, while their roles in pre-entry steps were examined using the EVA71 pseudoviral particles which only caused single round of infection. In both assays, the viral replication and infectivity could be easily monitored by luciferase activity or EGFP expression (Chen et al., 2012). Upon the VCP inhibition, we found that EVA71 replicon RNA activity was barely affected by NMS-873 during the early hours (translation phase) post transfection while it was suppressed at later time points (replicative phase) (Fig. 5d), consistent with early reports showing the involvement of VCP in enterovirus replications (Arita et al., 2012). In contrast, in the parallel EVA71 pseudovirus experiment, viral activity was significantly reduced from the very early phase of infection by NMS-873 treatment

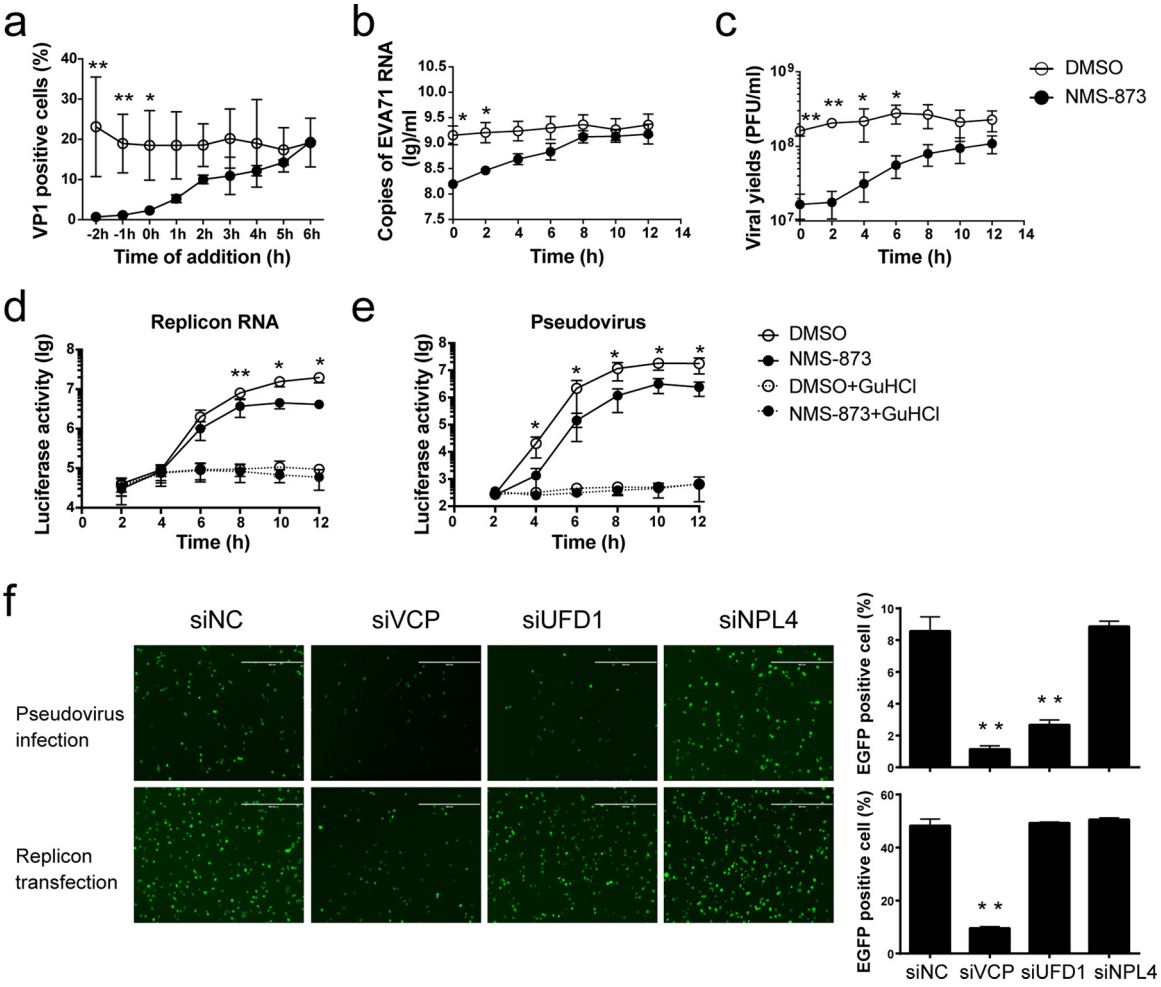

Fig. 5. UFD1 targets viral entry step but not replication during viral life cycle.

A. RD cells were infected with EVA71 at an MOI of 1, and then DMSO or NMS-873 (8 μM) was added at -2 h, -1 h, 0 h, 1 h, 2 h, 3 h, 4 h and 5 h. The cells were applied to flow cytometry at 6 hpi. EVA71 was added at 0 h. B–C. RD cells were incubated with EVA71 at an MOI of 10 at 37 °C for 1 h, and then the virus was removed. After extensive wash, cells were treated with DMSO or NMS-873 (8 μM) at 0, 2, 4, 6, 8 and 10 hpi. The total EVA71 RNA levels were determined by qPCR (B) and the viral yields were measured by plaque assay (C) at 12 hpi. D–E. RD cells were pretreated with DMSO, NMS-873 (8 μM), DMSO plus GuHCl (2 μM) or NMS-873 plus GuHCl for 30 min. Then cells were transfected with EVA71 replicon RNA (0.1 μg/well, D) or infected with EVA71 pesudovirus (25 μl/well, E). Luciferase activity was quantified at different time points post transfection or infection. F. RD cells were transfected with siRNA against VCP, UFD1 and NPL4. siNC was used as negative control. After 3 days, cells were transfected with EVA71-EGFP replicon RNA (0.1 μg/well) or infected with EVA71-EGFP pesudovirus (100 μl/well) for 12 h. EGFP expression was detected by fluorescence microscope and flow cytometry. All the experiments were repeated independently three times and shown as means ± SD. Statistical significance was determined by Student's *t* test Student's *t* test. *, $p < 0.05$; **, $p < 0.01$.

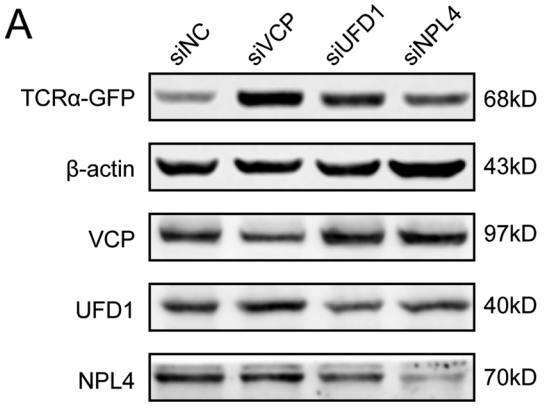

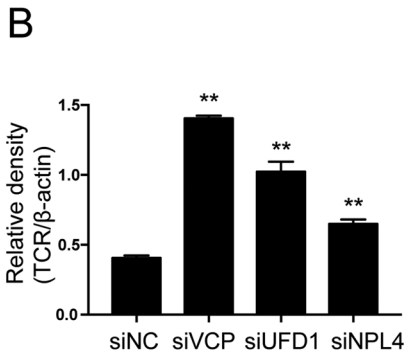

Fig. 6. VCP, UFD1 and NPL4 are critical for ERAD.

A–B. RD cells overexpressing TCRα-GFP were transfected with siRNA against VCP, UFD1 or NPL4. siNC was used as negative control. After 3 days, cells were lysed and probed with anti-GFP, VCP, UFD1 and NPL4 antibodies. β-actin was used as an internal control. The representative blots were shown (A). Three independent experiments were summarized as means ± SD (B). Statistical significance was determined by Student's *t* test Student's *t* test. *, $p < 0.05$; **, $p < 0.01$.

versus DMSO control group (Fig. 5e), indicating an early involvement.

Next, we utilized EGFP expressing EVA71 replicon and pseudovirus to examine the effect of VCP/UFD1 in viral replication and infection. We found that knockdown of VCP could significantly reduce EGFP expression both in replicon RNA transfection and pseudovirus infection. Surprisingly, although knockdown of UFD1 significantly decreased EGFP expression in pseudovirus assays, it barely inhibited viral activities in viral replication assays (Fig. 5f). This data suggests that UFD1 is involved specifically in the early stage of EVA71 life cycle, while VCP may play multiple roles at both pre-entry and post-entry levels.

3.6. UFD1 knockdown downregulated the nucleolin expression and reduced the binding of EVA71 to host cells

We further explored the working mechanisms of VCP-UFD1 during the early step of enterovirus life cycle. UFD1 and NPL4 were known to participate in the endoplasmic reticulum associated degradation (ERAD) process (Nowis et al., 2006). However, our data showed that UFD1 was involved in EVA71 infection and NPL4 was not, suggesting the mechanism may not be related to ERAD. To confirm this, we utilized the TCRα-GFP overexpressing RD cells in which overexpressed TCRα was degraded by ERAD, and disruption of ERAD led to TCRα accumulation. Indeed, VCP, UFD1 or NPL4 knockdown, which disrupts the ERAD processes, all significantly increased TCRα levels (Fig. 6a and b). In contrast, knockdown of VCP/UFD1 but not NPL4 decreased EVA71 infection. Therefore, we concluded that UFD1 facilitates EVA71 infection though a non-ERAD mediated process.

Next, we investigated whether UFD1 participated in viral binding and cellular uptake during the early stages of viral life cycle. We found that knockdown of VCP or UFD1 significantly decreased the binding and uptake of EVA71 to RD cells, but knockdown of NPL4 did not (Fig. 7a). This observation was further confirmed by confocal imaging assay showing less fluoresent-EVA71 binding to the cell surface of RD cells which were transfected with VCP or UFD1 siRNA, compared with NPL4 and control group (Fig. 7b). Consistent with reduced binding, the uptake of EVA71 by the infected cells showed the same decreasing trend, with significant inhibition by VCP or UFD1 siRNA but not by NPL4 (Fig. 7b).

It is unexpected to find that UFD1, an intracellular protein, affects the enterovirus binding to host cells. Therefore, we hypothesized whether UFD1 affected the expression of enterovirus receptors. We measured the expression levels of EVA71 uncoating receptor SCARB2 and binding receptors (Annexin A2, vimentin, nucleolin). Interestingly, the protein level of nucleolin was found significantly downregulated in VCP or UFD1 knockdown cell, whereas the expressions of all other receptors were barely affected (Fig. 8a). Knockdown of nucleolin did not affect the expression of UFD1 (Fig. 8b). We further confirmed that NMS-873 treatment also significantly reduced nucleolin levels but not the other receptors in RD cells (Fig. 8c). In addition, knockdown of nucleolin significantly reduced the infection of EVA71 (Fig. 8d).

We reasoned that VCP-UFD1 may affect the enterovirus binding through regulation of nucleolin levels. To test the significance of this VCP/UFD1-nucleolin axis for infection by other enterovirus species, we examined the effect of VCP, UFD1, NPL4 and nucleolin siRNA on EVA71 (*Enterovirus A* member), CVB3 (*Enterovirus B* member) and poliovirus (*Enterovirus C* member), we found that knockdown of VCP could significantly reduce the infection of EVA71 and poliovirus, but not CVB3 (Fig. 6E). In contrast, supporting the linkage of UFD1 and nucleolin, knockdown of either UFD1 of nucleolin affected the infection by EVA71, but not infections by CVB3 and poliovirus (Fig. 8e). These

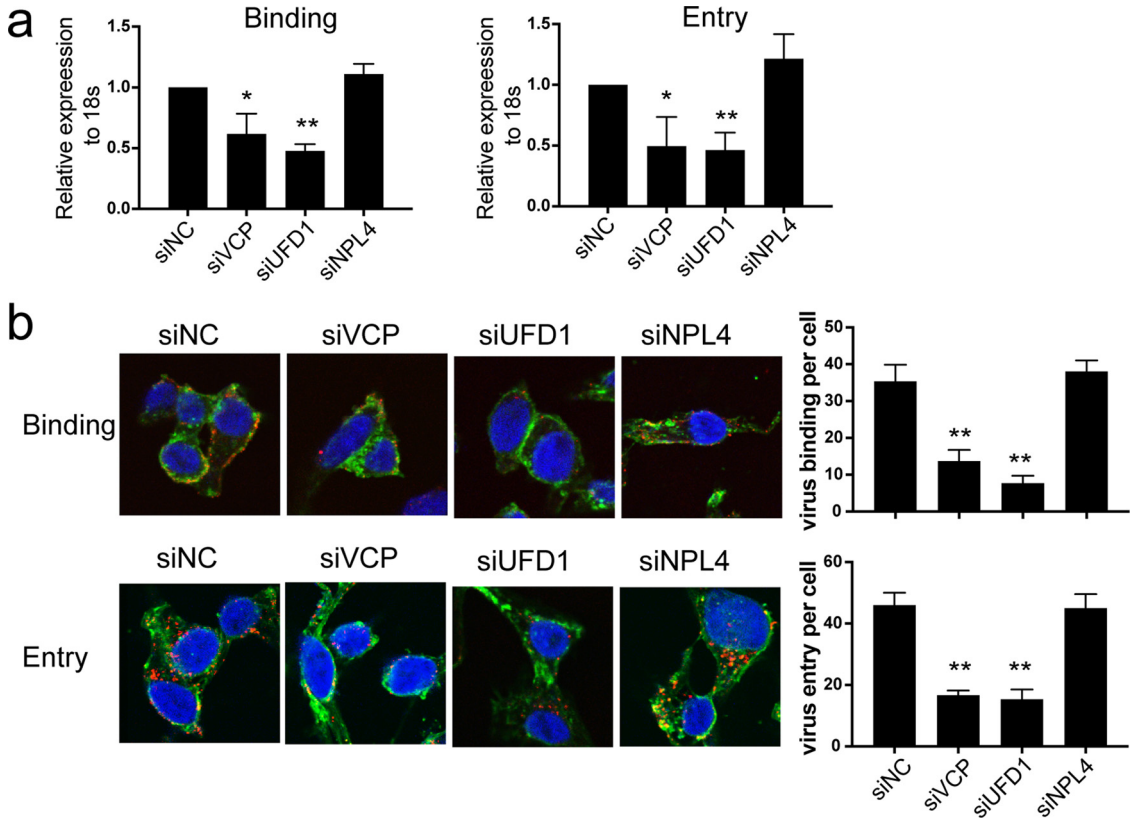

Fig. 7. Knockdown of UFD1 attenuates the binding and cellular uptake of EVA71 to host cells.
A–B. RD cells were transfected with siRNA against VCP, UFD1 and NPL4. siNC was used as negative control. After 3 days, cells were incubated with EVA71 (MOI = 10) at 4 °C (binding) or 37 °C (entry) for 2 h. After extensive wash, EVA71 RNA was detected by qPCR (A). Meanwhile, cells were incubated with EVA71-conjugated to AlexaFluor594 (MOI = 10) at 4 °C (binding) or 37 °C (entry) for 2 h. After extensive wash, EVA71 particles were detected by confocal microscope following WGA-AlexaFluor488 staining (B). Nuclei were stained by DAPI. (red, EVA71; green, membrane; blue, nuclei).

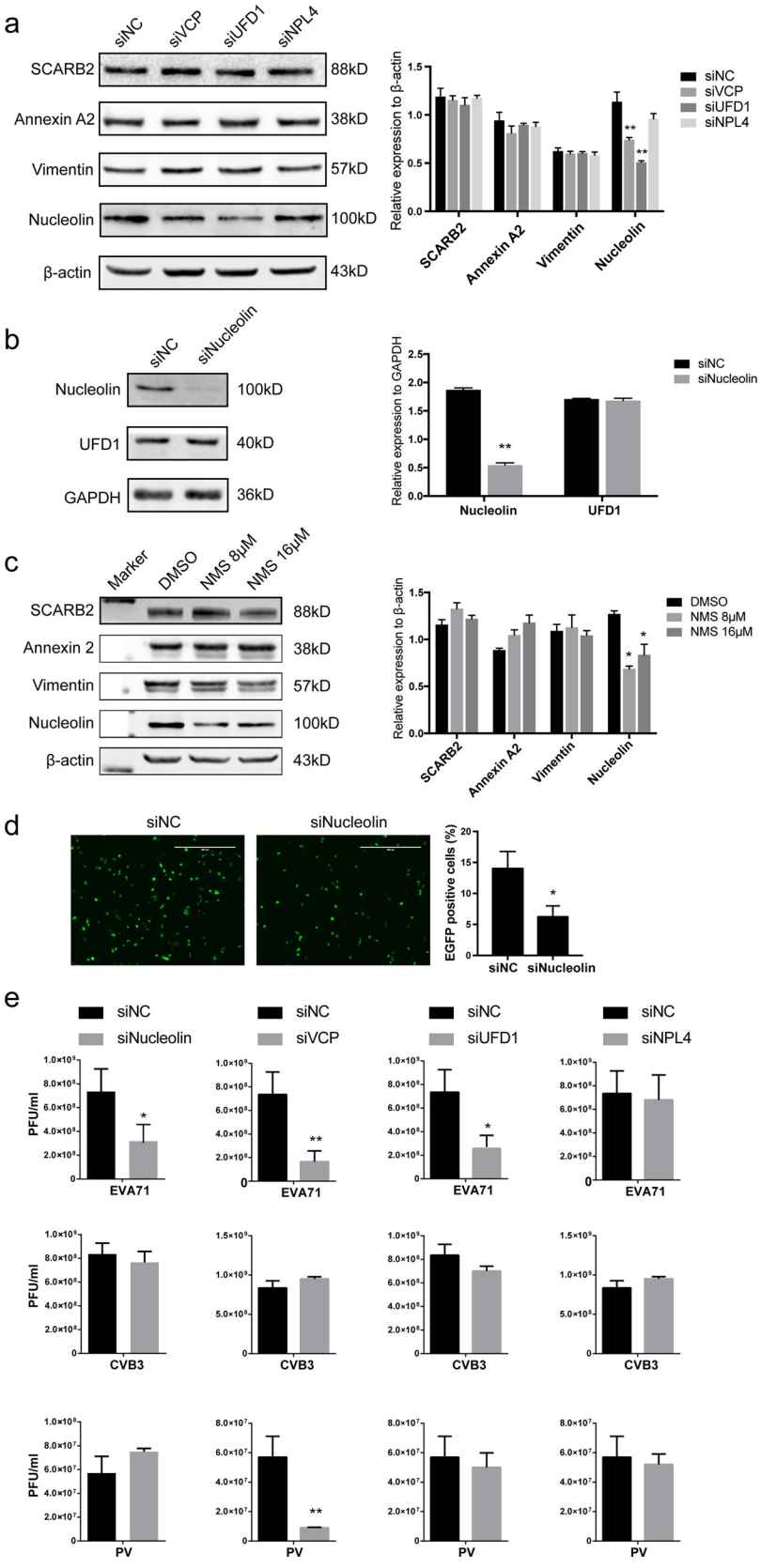

Fig. 8. VCP and UFD1 knockdown reduce the infection of EVA71 by modulating the expression of nucleolin.
A. RD cells were transfected with siRNA against VCP, UFD1 and NPL4. siNC was used as negative control. After 3 days, cells were lysed and probed with anti-SCARB2, Annexin A2, vimentin, nucleolin antibodies. β-actin was used as an internal control. The summarization of three independent experiments was shown at the right panel (means ± SD). B. RD cells were transfected with siRNA against nucleolin. siNC was used as negative control. After 3 days, cells were lysed and probed with anti-nucleolin and UFD1 antibodies. GAPDH was used as an internal control. The summarization of three independent experiments was shown at the right panel (means ± SD). C. RD cells were treated with DMSO or NMS-873 at 8 μM or 16 μM for 8 h. Then cells were lysed and probed with anti-SCARB2, Annexin A2, vimentin, nucleolin antibodies. β-actin was used as an internal control. The summarization of three independent experiments was shown at the right panel (means ± SD). D. RD cells were transfected with siRNA against nucleolin. siNC was used as negative control. After 3 days, cells were infected with EVA71-EGFP pesudovirus (100 μl/well) for 12 h. EGFP expression was detected by fluorescence microscope and flow cytometry. E. RD cells were transfected with siRNA against nucleolin, VCP, UFD1, NPL4 as well as negative control (siNC) and replated in 12 well plates after 48 h. The next day, serially diluted EVA71, CVB3 and PV were used to perform plaque assay. All the aforementioned experiments were repeated independently at least three times and shown as means ± SD accordingly. Statistical significance was determined by Student's *t* test Student's *t* test. *, $p < 0.05$; **, $p < 0.01$.

results indicated that the UFD1-nucleolin likely working in an axis specifically takes part in the infection of *Enterovirus A species* but not *B* or *C*.

4. Discussion

VCP participates in multiple cellular pathways to modulate cellular homeostasis and is involved in virus infection. Early studies have

reported that VCP participated in viral genome replication of poliovirus, hepatitis C virus and West Nile virus (Arita et al., 2012; Phongphaew et al., 2017; Yi et al., 2016). In addition, roles of VCP in early stages of viral infection have been reported for Coronavirus and Sindbis virus (Panda et al., 2013; Wong et al., 2015). VCP is also important for Rift Valley Fever virus (RVFV) egress and knockdown of VCP led to the intracellular accumulation of RVFV (Brahms et al., 2017). Recently, Wang et al. reported that EVA71 affected ERAD and VCP was hijacked in viral replication complex and important for virus replication (Wang et al., 2017). These studies suggested that VCP may participate in various steps of viral life cycle. In this study, we confirmed that VCP functioned at both the early and later stages of EVA71 life cycle, including enterovirus entry, genome replication and likely virion release.

The precise functions of VCP are determined by its cofactors, we screened their involvements in the enterovirus activity. Of the 31 cofactors, UFD1 was identified as a crucial factor for EVA71 infection. UFD1 and its partner NPL4 bind to VCP and form protein complexes involved in various protein-quality control processes, such as ERAD (Nowis et al., 2006). We hypothesized the enterovirus infection may not rely on these conventional roles of VCP and UFD1. Indeed, we found that knockdown of VCP, UFD1 and NPL4 prevented the degradation of TCRα by ERAD. However, knockdown of NPL4 failed to affect EVA71 infection, so the role of UFD1 and VCP in EVA71 infection is independent of NPL4 or ERAD. Furthermore, we also found similar roles of VCP and UFD1 in facilitating infection of other *e*nteroviruses, such as CVA16, CAV6 and CVA10, whereas knockdown of NPL4 did not affect viral infections. Thus, our data suggested a novel role of UFD1 in infections by enteroviruses.

Importantly, knockdown of UFD1 significantly reduced pseudovirus infection but not replicon RNA replication, while knockdown of VCP significantly suppressed both replicon and pseudovirus activities, indicating the specific roles of UFD1 in early steps of viral life cycle. Indeed, additional experiments confirmed that UFD1 affected the EVA71 binding and subsequent entry to host cells. We assumed that UFD1 affect the viral entry indirectly since UFD1 is localized in cytosol and cell nucleus. Interestingly, we found that VCP and UFD1 knockdown reduced nucleolin levels and inhibited EVA71 infection. These data indicate that UFD1 likely acts as an upstream regulator for nucleolin, a coreceptor for EVA71. We further showed the matching effects of UFD1 and nucleolin knockdown in infections by different *Enterovirus* species. While knockdown of either UFD1 or nucleolin inhibited *Enterovirus A* (EVA71) infections, it failed to affect both *Enterovirus B* (CVB3) and *Enterovirus C* (poliovirus) infections. These data increase our understanding of the specific pre-entry regulatory process of *Enterovirus A*. Revealing the exact mechanism of how VCP-UFD1 regulates nucleolin may reveal potential intervention targets for those enteroviruses.

VCP likely played multiple roles in EVA71 infection, both the pre-entry and the post-entry process. So far, the underlying mechanisms and the involved co-factors in these processes are still elusive. In the screening of cofactors, we identified that UBXN6 and SPRTN knockdown also had inhibitory effects on EVA71 infection. It has been reported that SPRTN is a regulator of UV-induced DNA damage response and promote ubiquitination of PCNA and synthesis of translesion DNA synthesis (Machida et al., 2012). UBXN6 is an ATP-driven separating enzyme which can remove misfolded proteins through ERAD pathway and promotes macrophage phagocytosis to remove damaged lysosomes (Nagahama et al., 2009; Papadopoulos et al., 2017; Trusch et al., 2015). We attempt to think that when viral RNA is released in the infected cell, VCP may collaborate with SPRTN or other unidentified factors to protect viral RNA from host sensing and degradation, thus promoting the replication and translation of viral RNA. Whereas VCP may recruit UBXN6 or other unknown factors, to participate in the ROs formation by dealing with the mis-assembled and misfolded proteins. These assumptions require future experimental validations and the results will lead to more insights of the versatile roles of VCP and its cofactors during viral infections.

In summary, based on the aforementioned results, we would like to propose the novel regulatory mechanism involving VCP-UFD1-Nucleolin axis which plays specific roles in infections by *Enterovirus A* species but not *B* or *C*. In this model, VCP associates with UFD1 to facilitate the binding of *Enterovirus A* serotypes to host cells through regulating the nucleolin levels, while VCP and other uncharacterized factors regulate more post-entry activities.

Funding

This work was supported in part by the National Basic Research Program of China (2015CB554300 to SZ), National Natural Science Foundation of China (81772181 to ZY) and Shanghai Municipal Commission of Health and Family Planning (20174Y0099 to JY).

CRediT authorship contribution statement

Jingjing Yan: Investigation, Methodology, Visualization, Writing - original draft. **Meng Wang:** Investigation, Methodology, Visualization. **Min Wang:** Methodology. **Ying Dun:** Validation. **Liuyao Zhu:** Validation. **Zhigang Yi:** Methodology, Resources, Writing - review & editing. **Shuye Zhang:** Supervision, Conceptualization, Methodology, Writing - original draft.

Declaration of Competing Interest

The authors declare no conflict of interest.

Acknowledgments

We thank Dr. Wenhui Li from NIBS for kindly providing the plasmids of EVA71 subgenomic replicon and EVA71 capsid. We thank Dr. Yunwen Hu and Zhigang Song from Shanghai Public Health Clinical Center for kindly providing the viruses of EVA71, CVA6 and CVA16. We also thank Dr. Chunsheng Dong from Soochow University for kindly providing the virus of CVB3.

References

Arita, M., Wakita, T., Shimizu, H., 2012. Valosin-containing protein (VCP/p97) is required for poliovirus replication and is involved in cellular protein secretion pathway in poliovirus infection. J. Virol. 86 (10), 5541–5553.

Arumughan, A., Roske, Y., Barth, C., Forero, L.L., Bravo-Rodriguez, K., Redel, A., Kostova, S., McShane, E., Opitz, R., Faelber, K., Rau, K., Mielke, T., Daumke, O., Selbach, M., Sanchez-Garcia, E., Rocks, O., Panakova, D., Heinemann, U., Wanker, E.E., 2016. Quantitative interaction mapping reveals an extended UBX domain in ASPL that disrupts functional p97 hexamers. Nat. Commun. 7, 13047.

Aswathyraj, S., Arunkumar, G., Alidjinou, E.K., Hober, D., 2016. Hand, foot and mouth disease (HFMD): emerging epidemiology and the need for a vaccine strategy. Med. Microbiol. Immunol. 205 (5), 397–407.

Baggen, J., Thibaut, H.J., Strating, J., van Kuppeveld, F.J.M., 2018. The life cycle of non-polio enteroviruses and how to target it. Nat. Rev. Microbiol. 16 (6), 368–381.

Brahms, A., Mudhasani, R., Pinkham, C., Kota, K., Nasar, F., Zamani, R., Bavari, S., Kehn-Hall, K., 2017. Sorafenib impedes rift valley fever virus egress by inhibiting valosin-containing protein function in the cellular secretory pathway. J. Virol. 91 (21).

Buchberger, A., Schindelin, H., Hanzelmann, P., 2015. Control of p97 function by cofactor binding. FEBS Lett. 589 (19 Pt A), 2578–2589.

Chen, P., Song, Z., Qi, Y., Feng, X., Xu, N., Sun, Y., Wu, X., Yao, X., Mao, Q., Li, X., Dong, W., Wan, X., Huang, N., Shen, X., Liang, Z., Li, W., 2012. Molecular determinants of enterovirus 71 viral entry: cleft around GLN-172 on VP1 protein interacts with variable region on scavenge receptor B 2. J. Biol. Chem. 287 (9), 6406–6420.

Cherry, S., Kunte, A., Wang, H., Coyne, C., Rawson, R.B., Perrimon, N., 2006. COPI activity coupled with fatty acid biosynthesis is required for viral replication. PLoS Pathog. 2 (10), e102.

Dang, M., Wang, X., Wang, Q., Wang, Y., Lin, J., Sun, Y., Li, X., Zhang, L., Lou, Z., Wang, J., Rao, Z., 2014. Molecular mechanism of SCARB2-mediated attachment and uncoating of EV71. Protein Cell 5 (9), 692–703.

DeLaBarre, B., Brunger, A.T., 2003. Complete structure of p97/valosin-containing protein reveals communication between nucleotide domains. Nat. Struct. Biol. 10 (10), 856–863.

Du, N., Cong, H., Tian, H., Zhang, H., Zhang, W., Song, L., Tien, P., 2014. Cell surface

vimentin is an attachment receptor for enterovirus 71. J. Virol. 88 (10), 5816–5833.
Du, X., Zhang, Y., Zou, J., Yuan, Z., Yi, Z., 2018. Replicase-mediated shielding of the poliovirus replicative double-stranded RNA to avoid recognition by MDA5. J. Gen. Virol. 99 (9), 1199–1209.
Hanzelmann, P., Schindelin, H., 2017. The interplay of cofactor interactions and post-translational modifications in the regulation of the AAA+ ATPase p97. Front. Mol. Biosci. 4, 21.
He, Q.Q., Ren, S., Xia, Z.C., Cheng, Z.K., Peng, N.F., Zhu, Y., 2018. Fibronectin facilitates enterovirus 71 infection by mediating viral entry. J. Virol. 92 (9).
Huang, H.I., Weng, K.F., Shih, S.R., 2012. Viral and host factors that contribute to pathogenicity of enterovirus 71. Future Microbiol. 7 (4), 467–479.
Machida, Y., Kim, M.S., Machida, Y.J., 2012. Spartan/C1orf124 is important to prevent UV-induced mutagenesis. Cell Cycle 11 (18), 3395–3402.
Magnaghi, P., D'Alessio, R., Valsasina, B., Avanzi, N., Rizzi, S., Asa, D., Gasparri, F., Cozzi, L., Cucchi, U., Orrenius, C., Polucci, P., Ballinari, D., Perrera, C., Leone, A., Cervi, G., Casale, E., Xiao, Y., Wong, C., Anderson, D.J., Galvani, A., Donati, D., O'Brien, T., Jackson, P.K., Isacchi, A., 2013. Covalent and allosteric inhibitors of the ATPase VCP/p97 induce cancer cell death. Nat. Chem. Biol. 9 (9), 548–556.
Meyer, H., Weihl, C.C., 2014. The VCP/p97 system at a glance: connecting cellular function to disease pathogenesis. J. Cell. Sci. 127 (Pt 18), 3877–3883.
Nagahama, M., Ohnishi, M., Kawate, Y., Matsui, T., Miyake, H., Yuasa, K., Tani, K., Tagaya, M., Tsuji, A., 2009. UBXD1 is a VCP-interacting protein that is involved in ER-associated degradation. Biochem. Biophys. Res. Commun. 382 (2), 303–308.
Nowis, D., McConnell, E., Wojcik, C., 2006. Destabilization of the VCP-Ufd1-Npl4 complex is associated with decreased levels of ERAD substrates. Exp. Cell Res. 312 (15), 2921–2932.
Owino, C.O., Chu, J.J.H., 2019. Recent advances on the role of host factors during non-poliovirus enteroviral infections. J. Biomed. Sci. 26 (1), 47.
Panda, D., Rose, P.P., Hanna, S.L., Gold, B., Hopkins, K.C., Lyde, R.B., Marks, M.S., Cherry, S., 2013. Genome-wide RNAi screen identifies SEC61A and VCP as conserved regulators of Sindbis virus entry. Cell Rep. 5 (6), 1737–1748.
Papadopoulos, C., Kirchner, P., Bug, M., Grum, D., Koerver, L., Schulze, N., Poehler, R., Dressler, A., Fengler, S., Arhzaouy, K., Lux, V., Ehrmann, M., Weihl, C.C., Meyer, H., 2017. VCP/p97 cooperates with YOD1, UBXD1 and PLAA to drive clearance of ruptured lysosomes by autophagy. EMBO J. 36 (2), 135–150.
Phongphaew, W., Kobayashi, S., Sasaki, M., Carr, M., Hall, W.W., Orba, Y., Sawa, H., 2017. Valosin-containing protein (VCP/p97) plays a role in the replication of West Nile virus. Virus Res. 228, 114–123.
Plevka, P., Perera, R., Cardosa, J., Kuhn, R.J., Rossmann, M.G., 2012. Crystal structure of human enterovirus 71. Science 336 (6086), 1274.
Su, P.Y., Wang, Y.F., Huang, S.W., Lo, Y.C., Wang, Y.H., Wu, S.R., Shieh, D.B., Chen, S.H., Wang, J.R., Lai, M.D., Chang, C.F., 2015. Cell surface nucleolin facilitates enterovirus 71 binding and infection. J. Virol. 89 (8), 4527–4538.
Trusch, F., Matena, A., Vuk, M., Koerver, L., Knaevelsrud, H., Freemont, P.S., Meyer, H., Bayer, P., 2015. The N-terminal region of the ubiquitin regulatory X (UBX) domain-containing protein 1 (UBXD1) modulates interdomain communication within the valosin-containing protein p97. J. Biol. Chem. 290 (49), 29414–29427.
Walker, P.J., Siddell, S.G., Lefkowitz, E.J., Mushegian, A.R., Dempsey, D.M., Dutilh, B.E., Harrach, B., Harrison, R.L., Hendrickson, R.C., Junglen, S., Knowles, N.J., Kropinski, A.M., Krupovic, M., Kuhn, J.H., Nibert, M., Rubino, L., Sabanadzovic, S., Simmonds, P., Varsani, A., Zerbini, F.M., Davison, A.J., 2019. Changes to virus taxonomy and the international code of virus classification and nomenclature ratified by the international committee on taxonomy of viruses (2019). Arch. Virol. 164 (9), 2417–2429.
Wang, X., Peng, W., Ren, J., Hu, Z., Xu, J., Lou, Z., Li, X., Yin, W., Shen, X., Porta, C., Walter, T.S., Evans, G., Axford, D., Owen, R., Rowlands, D.J., Wang, J., Stuart, D.I., Fry, E.E., Rao, Z., 2012. A sensor-adaptor mechanism for enterovirus uncoating from structures of EV71. Nat. Struct. Mol. Biol. 19 (4), 424–429.
Wang, T., Wang, B., Huang, H., Zhang, C., Zhu, Y., Pei, B., Cheng, C., Sun, L., Wang, J., Jin, Q., Zhao, Z., 2017. Enterovirus 71 protease 2Apro and 3Cpro differentially inhibit the cellular endoplasmic reticulum-associated degradation (ERAD) pathway via distinct mechanisms, and enterovirus 71 hijacks ERAD component p97 to promote its replication. PLoS Pathog. 13 (10), e1006674.
Wong, H.H., Kumar, P., Tay, F.P., Moreau, D., Liu, D.X., Bard, F., 2015. Genome-wide screen reveals valosin-containing protein requirement for coronavirus exit from endosomes. J. Virol. 89 (21), 11116–11128.
Wu, K.X., Phuektes, P., Kumar, P., Goh, G.Y., Moreau, D., Chow, V.T., Bard, F., Chu, J.J., 2016. Human genome-wide RNAi screen reveals host factors required for enterovirus 71 replication. Nat. Commun. 7, 13150.
Wu, X., Meng, Y., Wang, C., Yue, Y., Dong, C., Xiong, S., 2018. Semaphorin7A aggravates coxsackievirusB3-induced viral myocarditis by increasing alpha1beta1-integrin macrophages and subsequent enhanced inflammatory response. J. Mol. Cell. Cardiol. 114, 48–57.
Yamayoshi, S., Yamashita, Y., Li, J., Hanagata, N., Minowa, T., Takemura, T., Koike, S., 2009. Scavenger receptor B2 is a cellular receptor for enterovirus 71. Nat. Med. 15 (7), 798–801.
Yang, S.L., Chou, Y.T., Wu, C.N., Ho, M.S., 2011. Annexin II binds to capsid protein VP1 of enterovirus 71 and enhances viral infectivity. J. Virol. 85 (22), 11809–11820.
Ye, Y., Meyer, H.H., Rapoport, T.A., 2003. Function of the p97-Ufd1-Npl4 complex in retrotranslocation from the ER to the cytosol: dual recognition of nonubiquitinated polypeptide segments and polyubiquitin chains. J. Cell Biol. 162 (1), 71–84.
Yi, Z., Fang, C., Zou, J., Xu, J., Song, W., Du, X., Pan, T., Lu, H., Yuan, Z., 2016. Affinity purification of the hepatitis C virus replicase identifies valosin-containing protein, a member of the ATPases associated with diverse cellular activities family, as an active virus replication modulator. J. Virol. 90 (21), 9953–9966.
Yuan, M., Yan, J., Xun, J., Chen, C., Zhang, Y., Wang, M., Chu, W., Song, Z., Hu, Y., Zhang, S., Zhang, X., 2018. Enhanced human enterovirus 71 infection by endocytosis inhibitors reveals multiple entry pathways by enterovirus causing hand-foot-and-mouth diseases. Virol. J. 15 (1), 1.
Zhang, Y., Zhu, Z., Yang, W., Ren, J., Tan, X., Wang, Y., Mao, N., Xu, S., Zhu, S., Cui, A., Zhang, Y., Yan, D., Li, Q., Dong, X., Zhang, J., Zhao, Y., Wan, J., Feng, Z., Sun, J., Wang, S., Li, D., Xu, W., 2010. An emerging recombinant human enterovirus 71 responsible for the 2008 outbreak of hand foot and mouth disease in Fuyang city of China. Virol. J. 7, 94.
Zhou, D., Zhao, Y., Kotecha, A., Fry, E.E., Kelly, J.T., Wang, X., Rao, Z., Rowlands, D.J., Ren, J., Stuart, D.I., 2019. Unexpected mode of engagement between enterovirus 71 and its receptor SCARB2. Nat. Microbiol. 4 (3), 414–419.